

BeppoSAX Monitoring of the BL Lac Mkn 501

E. Pian^{1,2}, G. Vacanti³, G. Tagliaferri⁴, G. Ghisellini⁴,
L. Maraschi⁵, A. Treves⁶, C. M. Urry¹, F. Fiore⁷, P. Giommi⁷,
E. Palazzi¹, L. Chiappetti⁸, R. M. Sambruna⁹

¹ STScI, 3700 San Martin Drive, Baltimore MD 21218

² ITESRE-CNR, via P. Gobetti 101, I-40129 Bologna, Italy

³ ESA ESTEC, Space Science Department, Astrophysics Division, Postbus 299, NL-2200 AG Noordwijk, The Netherlands

⁴ Osservatorio Astronomico di Brera, Via Bianchi 46, I-22055 Merate (Lecco), Italy

⁵ Osservatorio Astronomico di Brera, Via Brera 28, I-20121 Milan, Italy

⁶ Department of Physics, University of Milan at Como, Via Lucini 3, I-22100 Como, Italy

⁷ SAX SDC, Via Corcolle 19, I-00131, Rome, Italy

⁸ IFCTR-CNR, Via Bassini 15, I-20133 Milan, Italy

⁹ NASA/Goddard Space Flight Center, Greenbelt, MD 20771

Abstract.

The BL Lac object Mkn 501 was observed with the BeppoSAX satellite on 7, 11, and 16 April 1997 during a phase of high activity at TeV energies, as monitored with the Whipple, HEGRA and CAT Cherenkov telescopes. Over the whole 0.1-200 keV range the spectrum was exceptionally hard ($\alpha \leq 1$, with $F_\nu \propto \nu^{-\alpha}$) indicating that the X-ray power output peaked at (or above) ~ 100 keV. This represents a shift of at least two orders of magnitude with respect to previous observations of Mkn 501, a behavior never seen before in this or any other blazar. The overall X-ray spectrum hardens with increasing intensity and, at each epoch, it is softer at larger energies. The correlated variability from soft X-rays to the TeV band points to models in which the same population of relativistic electrons produces the X-ray continuum via synchrotron radiation and the TeV emission by inverse Compton scattering of the synchrotron photons or other seed photons.

INTRODUCTION

Mkn 501, one of the closest ($z=0.034$) BL Lacertae objects, and one of the brightest at all wavelengths, was the second source, after Mkn 421, to

be detected at TeV energies by the Whipple and HEGRA observatories [1,2]. Historically its spectral energy distribution (νF_ν) resembles that of BL Lac objects selected at X-ray energies (or HBL [3]), having a peak in the EUV-soft X-ray energy band. Accordingly, the 2–10 keV spectra observed so far were relatively steep, with energy spectral indices α larger than unity ($F_\nu \propto \nu^{-\alpha}$). From the EXOSAT data base the hardest X-ray spectrum of Mkn 501, observed in one of its brightest states, had a spectral index of 1.2 ± 0.1 [4]. *Einstein* measured in two occasions spectral indices consistent with values smaller than 1 within the large errors [5].

Mkn 501 was observed with BeppoSAX [6] over a period of ~ 10 hours on each 7, 11, and 16 April 1997, during a multiwavelength campaign involving ground-based TeV Cherenkov telescopes (Whipple, HEGRA and CAT), plus other satellites, CGRO (EGRET and OSSE), RXTE, ISO and optical telescopes. In this paper we briefly report the BeppoSAX results and their implications for blazar models, deferring to a separate paper [7] for an exhaustive presentation.

OBSERVATIONS, ANALYSIS, AND RESULTS

Event files for the LECS (0.1–10 keV), and the three MECS (1.5–11 keV) experiments were linearized and cleaned with SAXDAS; light curves and spectra were accumulated for each pointing with the SAXSELECT tool, using 8.5 and 4 arcmin extraction radii for the LECS and the MECS, respectively, that provide more than 90% of the fluxes. For the background subtraction we used the files accumulated from blank fields available from the BeppoSAX Science Data Center (SDC) public ftp site. Source+background and background spectra were accumulated for each of the four PDS units (15–300 keV), using the XAS software package. The source was significantly detected up to the highest energy channels. Each net spectrum was binned in energy intervals to reach a signal-to-noise ratio larger than 20, up to 150 keV. The grouped spectra from the four units were then coadded for each pointing.

Spectral analysis was performed with the XSPEC 9.01 package, using the response matrices released by the SDC. For each observation, the LECS and MECS spectra have been jointly fit with both a simple and a broken power-law model. The latter yields a better representation of the data, and a fitted N_{H} closer to the Galactic value [8]. We then fixed N_{H} at the Galactic value, and determined under this assumption the best-fit parameters for the broken power-law model. The spectral indices below and above the break energy of ~ 2 keV, respectively, are 0.63 ± 0.04 , 0.91 ± 0.02 (7 Apr), 0.64 ± 0.04 , 0.80 ± 0.02 (11 Apr), 0.40 ± 0.04 , 0.59 ± 0.02 (16 Apr). Single power-law fits to the PDS data in the 20–200 keV range give a good representation of the spectra. The spectral indices are 0.98 ± 0.13 (7 Apr), 0.79 ± 0.09 (11 Apr), 0.84 ± 0.04 (16 Apr). At each epoch the overall X-ray spectrum is softer at higher energies

and in each band hardens with increasing intensity (see Figure 1).

DISCUSSION

In Figure 1 the unfolded and unabsorbed X-ray spectra from the first and last BeppoSAX observations are compared with previously observed X-ray spectra [4] and with data in the radio [9], mm [10–13], far-infrared [14], optical [15,16], UV [17]; TeV-rays [1,2,18] (squares). Nearly simultaneous Whipple TeV data [19] are indicated as filled circles, while the open circle (13 April) and the TeV fitting curve along with its $1\text{-}\sigma$ confidence range (15–20 March) are from the HEGRA experiment [20].

The present X-ray observations imply a dramatic hardening of the spectral energy distribution in the medium X-ray band and an increase of the (apparent) bolometric luminosity of a factor ≥ 20 with respect to previous epochs. The really striking feature is that the peak of the power output is found to *shift* in energy by a factor ≥ 100 . Moreover for the first time in any object the peak is observed to *occur in the hard X-ray range*, definitely above $\sim 50 - 100$ keV. Since in the optical the source was nearly normal [21] the change of the spectral energy distribution seems to be confined to energies greater than ~ 0.1 keV, as also indicated by the apparent pivot of the three BeppoSAX spectra.

The overall continuity of the X-ray spectra presently observed with previous UV and soft X-ray measurements suggests that the X-ray emission constitutes the high energy end of the synchrotron component and thus that its peak frequency (i.e., where $\alpha = 1$) increased by more than two orders of magnitude with respect to previous observations of Mkn 501.

The TeV emission also brightened by more than a factor of 5 in the first two weeks of April, with the most intense TeV flare peaking on 16 April [19], the date of the last BeppoSAX observation. However, unlike the X-ray spectrum, the TeV spectrum was rather steep ($\alpha \simeq 1.5$) and did not show noticeable temporal variation [20,22].

The synchrotron self-Compton [23–25] model explains naturally the correlated flaring at X-ray and TeV energies if the energy distribution of the emitting electrons, $N(\gamma)$, changes at the highest energies. In fact the highest energy electrons produce X-rays via synchrotron and the TeV radiation via inverse Compton scattering. Due to the very high electron energies involved, the scattering cross section for energetic photons is reduced by the Klein-Nishina effect and only photons below the Klein-Nishina threshold ($h\nu \leq mc^2/\gamma$) are effectively upscattered. Therefore a) the inverse Compton flux does not vary more than the synchrotron flux, as it would normally be observed; b) the peak of the inverse Compton power shifts in frequency less than the synchrotron peak when the critical electron energy changes.

The shift of $\sim 2\text{--}3$ orders of magnitude in the frequency ν_S of the synchrotron peak cannot be ascribed to either a variation of Doppler factor δ or mag-

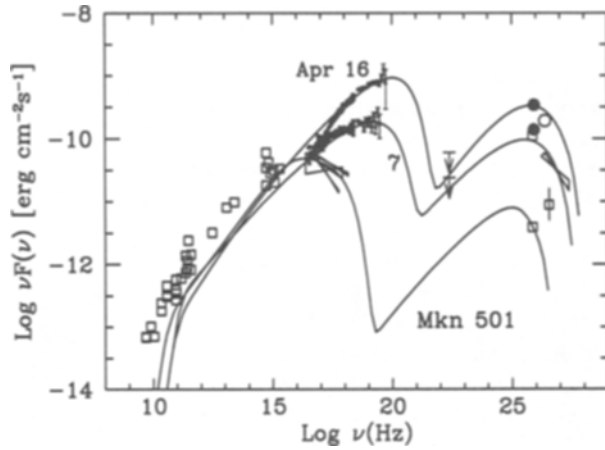


FIGURE 1. Spectral energy distribution of Mkn 501. See text for the data points. The solid lines indicate fits with a one-zone, homogeneous synchrotron self-Compton model: in the “quiescent state” the electrons are continuously injected with a power-law distribution ($\propto \gamma^{-2}$) between $\gamma_{min} = 2 \times 10^4$ and $\gamma_{max} = 4 \times 10^5$. For the fit to the 7 April spectrum the injected electron distribution ($\propto \gamma^{-1.4}$) extends from $\gamma_{min} = 1$ and $\gamma_{max} = 4 \times 10^6$. For the fit to the 16 April spectrum, the injected electron distribution ($\propto \gamma^{-1.1}$) extends from $\gamma_{min} = 1$ and $\gamma_{max} = 8 \times 10^6$. For all models, the beaming factor is $\delta = 10$ and the magnetic field $B \sim 0.5$ Gauss.

netic field B alone (enormous variations would be demanded, since $\nu_S \propto B\delta$). Therefore a real change in power is implied. Assuming that the variation is only due to a change in the electron energy, this must have increased by roughly a factor of ~ 10 – 30 . The corresponding shift of the inverse Compton peak is expected to be a factor of ~ 10 – 30 , in the linear Klein-Nishina regime. Since the cooling time of these very high energy electrons is rather short and the synchrotron peak did not move back to the quiescent position during at least 10 days, a mechanism of continuous particle injection is required.

Three simple, one-zone synchrotron self-Compton models along these lines are shown in Figure 1 for the quiescent state and the 7 and 16 April states of Mkn 501. The $N(\gamma)$ distribution has been found self-consistently solving the continuity equation including continuous injection of relativistic particles, radiative losses, electron-positron pair production and taking into account the Klein-Nishina cross section [26]. The parameters of the fits are given in the figure caption. A variation of the maximum energy of the emitting electrons, together with an increased luminosity and a flattening of the injected particle distribution can describe the observed spectra quite well. We have also assumed that the region where the variable and dominant X-ray and TeV flux is produced is more compact than the region responsible for the “quiescent” spectrum, but characterized by the same beaming factor and magnetic field.

REFERENCES

1. Quinn, J., et al. 1996, *ApJ*, 456, L83
2. Bradbury, S. M., et al. 1997, *A&A*, 320, L5
3. Padovani, P., & Giommi, P. 1995, *ApJ*, 444, 567
4. Sambruna, R. M., et al. 1994, *ApJS*, 95, 371
5. Urry, C. M., Mushotzky, R. F., & Holt, S. S. 1986, *ApJ*, 305, 369
6. Boella, G., et al. 1997, *A&AS*, 122, 299
7. Pian, E., et al. 1997, *ApJL*, submitted
8. Elvis, M., Lockman, F. J., & Wilkes, B. J. 1989, *AJ*, 97, 777
9. Gear, W. K., et al. 1994, *MNRAS*, 267, 167
10. Steppe, H., et al. 1988, *A&AS*, 75, 317
11. Wiren, S., Valtaoja, E., Teräsanta, H., & Kotilainen, J. 1992, *AJ*, 104, 1009
12. Lawrence, A., et al. 1991, *MNRAS*, 248, 91
13. Bloom, S. D., & Marscher, A. P. 1991, *ApJ*, 366, 16
14. Impey, C. D., & Neugebauer, G. 1988, *AJ*, 95, 307
15. Véron-Cetty, M.-P., & Véron, P. 1993, ESO Scientific Report No. 13, 1
16. Burbidge, G., & Hewitt, A. 1987, *AJ*, 93, 1
17. Pian, E., & Treves, A. 1993, *ApJ*, 416, 130
18. Weekes, T. C., et al. 1996, *A&AS*, 120, 603
19. Catanese, M., et al. 1997, *ApJ*, submitted
20. Aharonian, F., et al. 1997, *A&A*, submitted
21. Buckley, J., & McEnery, J. 1997, in preparation
22. Aharonian, F., et al. 1997, in Proc. of the 4th Compton Symposium, Williamsburg, 27-30 April 1997, in press
23. Jones, T. W., O'Dell, S. L., & Stein, W. A. 1974, *ApJ*, 188, 353
24. Ghisellini, G., Maraschi, L., & Dondi, L. 1996, *A&AS*, 120, 503
25. Mastichiadis, A., & Kirk, J. G. 1997, *A&A*, 320, 19
26. Ghisellini, G. 1989, *MNRAS*, 236, 341